



Published in final edited form as:

Nat Med. 2011 February ; 17(2): 216–222. doi:10.1038/nm.2290.

The Ngal Reporter Mouse Detects the Response of the Kidney to Injury in Real Time

Neal Paragas^{*,1}, Andong Qiu^{1,*}, Qingyin Zhang¹, Benjamin Samstein¹, Shi-Xian Deng¹, Kai M. Schmidt-Ott², Melanie Viltard¹, Wenqiang Yu¹, Catherine S. Forster¹, Gangli Gong¹, Yidong Liu¹, Ritwij Kulkarni¹, Kiyoshi Mori³, Avtandil Kalandadze¹, Adam J. Ratner¹, Prasad Devarajan, Donald W. Landry¹, Vivette D'Agati¹, Chyuan-Sheng Lin¹, and Jonathan Barasch^{†,1}

¹College of Physicians and Surgeons of Columbia University New York, N.Y. 10032

²Max-Delbruck Center for Molecular Medicine Berlin, Germany

³Kyoto University Graduate School of Medicine, Kyoto, Japan

Abstract

Many proteins have been proposed to act as surrogate markers of organ damage, yet for many candidates the essential characteristics which link the protein to the injured organ have not yet been described. We generated an NGAL-reporter mouse by inserting a di-fusion reporter gene, *Luciferase2(Luc2)/mCherry(mC)* into the *Ngal* locus. The *Ngal-Luc2/mC* reporter accurately recapitulated the endogenous message and illuminated injuries *in vivo* in real-time. In the kidney, *Ngal-Luc2/mC* imaging showed a sensitive, rapid, dose-dependent, reversible, and organ and cellular specific relationship with tubular stress, which quantitatively paralleled urinary Ngal (uNgal). Unexpectedly, specific cells of the distal nephron were the source of uNgal. Cells isolated from *Ngal-Luc2/mC* mice could also track both the onset and the resolution of the injury, and monitor the actions of NF- κ B inhibitors and antibiotics in the case of infection. Accordingly, the imaging of *Ngal-Luc2/mC* mice and cells identified injurious and reparative agents which effect kidney damage.

Introduction

Organ damage induces the appearance of many different proteins in serum and in urine, and some of these have been proposed to serve as surrogate measures of tissue damage. However, a “biomarker” must meet a number of criteria: (1), the protein must originate from injured, rather than from uninjured “bystanders” (2), the amount of the protein in the

Users may view, print, copy, download and text and data- mine the content in such documents, for the purposes of academic research, subject always to the full Conditions of use: http://www.nature.com/authors/editorial_policies/license.html#terms

[†]Corresponding Author: Columbia University, 630 West 168th St, New York, NY 10032, T: 212-305-1890, F: 212-305-3475, jmb4@columbia.edu.

Author Contribution

NP, AQ, CSL created the NGAL-Reporter Mouse, QZ and BS performed surgeries, SXD, GG, YL, DWL created NF κ B inhibitors, NP, RK and AJR studied bacteria induced NGAL expression, VD evaluated the pattern of NGAL expression, KMSO, MV, WY, CSF, KM, AK, and PD analyzed data. NP, AQ and JB and wrote the paper. AQ, NP and JB invented the luminescent mouse.

*Equal Contribution

biofluid must be proportional to its expression in the injured organ, and this quantity should reflect a graded, dose-dependent response to damage; (3), the biomarker should be temporally related to the inciting stimulus, so as to alert the clinician to a potentially reversible stage of the illness; (4), the expression of the biomarker should rapidly decay when the acute phase of injury has terminated; (5), the expression of the protein should be conserved across many patient populations and various animal models; (6), the biomarker should be a critical component of organ pathophysiology.

While studies have demonstrated the statistical power of different biomarkers, many candidates have yet to fulfill even the most basic concern that their serum or urine concentration is proportional to their expression at the site of injury *in vivo*. These data could be obtained by longitudinal measurements in the damaged organ itself and in the biofluid, but current methodology has been limited to intermittent sampling, which cannot convincingly associate organ injury with biofluid measurements. In addition, candidate biomarkers which are expressed in multiple organs must be investigated with tissue specific knockouts to associate the biomarker with the specific organ. Hence, a new technology is required for repetitive real time analysis of the injured organ and the biofluid.

The current diagnosis of acute kidney injury (AKI) relies not on the measurement of a marker of acute injury, but instead on a marker of steady state kidney function, called muscle-derived serum creatinine (sCr). In non-steady state conditions, such as AKI, however, sCr is a retrospective, insensitive, and even a deceptive measure of kidney injury. sCr is retrospective because it must accumulate over many days, a delay which is subject to extra-renal modifiers such as muscle mass and diet¹. The marker is insensitive because even a 50% loss of renal function may be required to elevate sCr sufficiently to come to medical attention, whereas levels which fall short of this threshold are usually dismissed, despite their known association with excess mortality and prolonged hospitalization². sCr is deceptive because its level often reflects transient physiologic adaptations to volume changes or the presence of chronic kidney disease (CKD), rather than AKI. Most importantly, the measurement of sCr fails to identify the cell type which is acutely injured, albeit that this localization critically determines the natural history of the disease and its response to therapy³. These data call for new methods which can identify injured cells in the initial phases of AKI.

NGAL was first reported in ischemic kidneys using gene arrays⁴ and then in hospitalized patients using immunoblots⁵. Subsequent studies in adults⁶, children⁷, mice^{5,8}, rats, and pigs have shown that serum and urine Ngal (sNgal and uNgal, respectively) are up regulated in the biofluid after ischemia-reperfusion injury, hypoxia, drug toxicity, and bacterial infections^{5,8,9} before sCr is elevated. However, like most candidate biomarkers, the source of the protein, its relationship to damage *in vivo*, and the mechanisms of its expression are poorly defined, necessitating animal models to resolve these fundamental issues.

To understand whether Ngal protein fulfills the criteria of a biomarker, we developed a reporter mouse to compare the time course of *Ngal* gene and protein expression *in vivo*. Using this model, we investigated the sensitivity, kinetics, dose-dependency, reversibility

and organ and cellular specificity of Ngal expression. Real time imaging identified the pathways that activate *Ngal* and the site of injury where kidney *Ngal* produces uNgal.

Results

Generation of the *Ngal* di-fusion reporter mouse

The *Ngal* di-fusion reporter mouse was generated by knocking a di-fusion reporter gene consisting of Luciferase 2 (*Luc2*) and mCherry (*mC*) into a site between the 5' UTR and the start codon of the *Ngal* gene, hence driving the di-fusion reporter with the endogenous *Ngal* promoter and its 5' UTR (Supplementary Fig. 1). The construct, an in-frame ligation of *Luc2* and *mC* ORFs (Supplementary Table 1), was functionally tested by transient expression in HeLa cells (Supplementary Fig. 2) prior to BAC recombineering (Supplementary Fig. 1a). *Ngal*-targeted kv1 ES cells (Supplementary Fig. 1c, Supplementary Fig. 3) upregulated expression of *Ngal-Luc2/mC* in response to treatment with sodium cyanide (1 mM) or lipid A (4 µg/ml), demonstrating the functionality of the knockin. The F1 heterozygous *Ngal-Luc2/mC* mice were identified by PCR-genotyping (Supplementary Fig. 1b, d), by Long-distance PCR (Supplementary Fig. 1b, e) and by DNA sequencing of the integration sites.

Ngal-Luc2/mC mouse reports ischemia and lipid A induced kidney injury

Unilateral ischemia (I/R, 15 or 30min) in either the right or the left kidney of either male or female mice induced *Ngal-Luc2/mC* activity specifically in the operated kidney ($n=8$; Fig. 1a, Supplementary Fig. 4). In contrast, the contra-lateral kidney and the extra-renal organs did not express high levels of *Ngal-Luc2/mC*. The specificity of the reporter was confirmed in sectioned kidneys which emitted luminescence from the medulla of the injured kidney (Fig. 1b) (12h after 30min ischemia) but not from the contralateral, uninjured kidney (Fig. 1b).

The time course of *Luc2/mC* expression was visualized in living mice. We found markedly increased bioluminescence and fluorescence (~10 fold increase) 3–6h after renal artery clamping (Fig. 1a, c, Supplementary Fig. 4a) and peak expression (~25–80 fold increase) was found 12h after ischemia (Fig. 1c, Supplementary Fig. 4a). The intensity of the response depended on the ischemic dose: for example, *NGAL-Luc2* activity rose 25- or 70-fold, after a 15min or a 30min dose of ischemia, respectively (Fig. 1c). Kidney *Ngal-Luc2* and uNgal were strictly correlated, both temporally and in the intensity of their responses, implying that the protein originated from the kidney (Fig. 1d, Supplementary Fig. 4b).

Because sCr was unchanged in unilateral kidney injury, we compared *Ngal-Luc2/mC* and sCr in bilateral I/R (Fig. 1e–g, Supplementary Figure 5a). In this model, *Ngal-Luc2* (Fig. 1f) and uNgal expression (Fig. 1g) consistently rose between 3 and 6h after ischemia, but sCr lagged by 12h (Fig. 1f) and additionally significant changes in uCr were detectable only when urine collections occurred in 3h intervals. The data demonstrate that *NGAL-Luc2/mC* and uNgal were more sensitive, rapid, and dynamic measures of AKI than were sCr and uCr¹⁰, confirming our earlier work in mice⁸ and humans^{6,11}. Likewise other biomarkers such as N-acetyl-beta-D-glucosaminidase were delayed (not shown).

Next we examined whether Ngal-Luc2/mC reported nephrotoxic damage. Kidney Ngal-Luc2/mC and uNgal (Fig. 2a, b) were markedly upregulated after exposure to cisplatin (20 mg/kg). Cells extracted from Ngal-Luc2/mC kidneys also responded to cisplatin (10 μ M) (Fig. 2c) implying a direct effect. Lipid A (*i.p.*), the purified lipid component of endotoxin induced dose-dependent increases in Ngal-Luc2/mC expression (5, 15 and 30 lipid A (mg/kg) induced 17.3, 21.5 and 33.9 fold increases in Ngal-Luc2, respectively; $n=6$) in many organs including kidney, liver, and lung (Fig. 2d). Kidney Ngal-Luc2 was most pronounced at 30 mg/kg lipid A, consistent with a dose-dependent increase in sCr (Fig. 2e). Lung Ngal-Luc2 was most pronounced when lipid A was aspirated (Supplementary Fig. 5b), producing a typical luminescent pattern¹². Hence, while we found little expression of Ngal-Luc2/mC outside of the kidney in response to cisplatin and non-uremic I/R¹³, *Ngal-Luc2/mC* could also detect the effect of toxins that injure multiple organs.

The kidney is the source of urinary NGAL (uNgal)

uNgal has been used as a quantitative surrogate for kidney NGAL, but no experimental evidence has validated this linkage. Although kidney Ngal-Luc2/mC and uNgal were expressed simultaneously, it could not be concluded that the kidney was the major source of uNgal.

To examine whether uNgal originated in the kidney, we performed kidney cross-transplants between *Ngal* knockout (*Ngal*^{-/-}) and wild type C57BL/6 mice (*Ngal*^{+/+}), followed by renal artery clamping (10min). There was a 228.1 \pm 18.8 fold, and a 184.6 \pm 56.7 fold induction of *Ngal* mRNA (QPCR) in ischemic wild type kidneys (respectively, *Ngal*^{+/+} kidneys transplanted into *Ngal*^{+/+} hosts, $n=6$ and *Ngal*^{+/+} kidneys into *Ngal*^{-/-} hosts, $n=4$), whereas there was only a 6.3 \pm 0.86 fold *Ngal* induction in the ischemic knockout kidney (*Ngal*^{-/-} kidneys into *Ngal*^{+/+} hosts, $n=5$) (Supplementary Fig. 6a). Consistently, uNgal protein rose in *Ngal*^{+/+} kidneys transplanted to *Ngal*^{+/+} or *Ngal*^{-/-} hosts, whereas smaller increases in uNgal were found in *Ngal*^{-/-} kidneys transplanted to *Ngal*^{+/+} hosts ($P<0.005$ at 12h and $P<0.02$ at 24h; Supplementary Fig. 6b). Infiltrating RNA⁺ cells or small amounts of sNgal might explain the small amount of uNgal in *Ngal*^{-/-} kidney recipients, the former explanation more tenable because NGAL message was detected in *Ngal*^{-/-} kidneys, and after I/R, less serum ²⁵I-sNgal (0.21 \pm 0.04 fold less; 1 μ g, *i.p.*) reached the urine than in un-operated mice. In all of the cross-transplants, *Kim1*, a biomarker of AKI, was upregulated after ischemia (~9 fold) confirming kidney injury. In contrast, liver NGAL was not activated, demonstrating the specificity of the surgical manipulation. Likewise, but deletion of neutrophils¹⁴ by RB-6 antibodies (Supplementary Fig. 7) failed to alter expression of kidney *Ngal*. Taken together with the specific expression of kidney Ngal-Luc2/mC in surgical models, and the strict correlation between kidney and urinary Ngal kinetics, these studies indicate that uNgal originates predominately from kidney epithelia.

The damaged nephron is the source of *Ngal* in the kidney

To determine the cellular source of Ngal, we dissected reporter kidneys 24h after I/R (15min dose). As shown in Fig. 3, Supplementary Figs. 8-10 *Ngal* RNA and mC fluorescence was expressed by the Thick Ascending Limbs of Henle (TAL), the macula densa (MD), and the intercalated cells (IC) of the collecting ducts (CD) after ischemia. The distal convoluted

tubule (DCT) also expressed *Ngal* but at a lower level, and no expression was found in proximal tubules (PT) (Fig. 3a–d). By co-staining the hybridization with v-ATPase B1/2 antibodies, we found that α -type IC cells (apical v-ATPase) expressed *Ngal* (Fig. 3e–g). A very similar pattern of *Ngal* expression was also found in the kidney after treatment with lipid A (15mg/kg), except that inner medullary tubules were accentuated (Fig. 2f, g), perhaps due to the local concentration of lipid A or TLR receptors^{15,16}. Obstruction of the ureter also induced *Ngal* expression in inner medullary tubules (Supplementary Fig. 8d).

Next, we examined whether *Ngal* originated from injured nephrons or from adjacent uninjured bystanders. We did this by comparing *Ngal* with post-ischemic (30min ischemia; Jablonski score of 3) or post-lipid A tubular morphology. *Ngal* was found in tubules in the outer strip of the outer medulla, which generally showed dilation and attenuation or intraluminal debris or casts (Fig. 2g, 3b–f). When we clamped a polar (segmental) artery for 30min, cast-filled inner medullary tubules expressed *Ngal*, whereas tubules in the non-ischemic domain did not express *Ngal* (Fig. 3h, i). In summary, *Ngal* expression appeared specifically in distal tubular segments of injured nephrons, but it was not expressed in non-ischemic zones.

Ngal-Luc2/mC expression distinguishes volume depletion from AKI

Volume depletion (pre-renal azotemia) is a physiological adaptation characterized by few anatomical changes, but which confuses the diagnosis of AKI by elevating sCr. We found that mild pre-renal azotemia produced hypernatremia (140.3±1.5 to 148.3±2.5 mmol/L; $n=3$), reduced body weight (21.7±4%), and caused a small rise in sCr (0.3±0.2 mg/dL), but failed to induce Ngal-Luc2/mC ($n=3$; Fig. 4). Hence Ngal-Luc2/mC distinguished AKI from volume depletion consistent with human studies⁶.

Expression of Ngal visualizes pharmacological interventions

Uropathogenic *E. coli* are the principal cause of urogenital infection. Since *Ngal* is a bacteriostatic protein mediating innate immune responses by sequestering iron from bacteria¹⁷, we tested whether *Ngal* responded to *E. coli* CFT073¹⁸. As shown in Fig. 5a, Ngal-Luc2 was upregulated by CFT073 (2.9±0.4 fold; $P=0.042$) in primary *Ngal-Luc2/mC* kidney cells, correlating with bacterial counts (data not shown). Brief treatment with gentamicin (100 μ g/ml) suppressed the Ngal-reporter (no antibiotic vs antibiotic, $P=0.034$), particularly when gentamicin was used as a pre-treatment, rather than after bacterial growth.

Uropathogenic bacteria activate NF- κ B signaling by binding to TLRs such as TLR4⁸. Because previous studies suggested that *Ngal* was a potential target of NF- κ B¹⁹, we determined whether *Ngal* could be suppressed by blocking NF- κ B. As shown in Fig. 5b, lipid A (4 μ g/ml) activated NGAL-Luc2 (1.97±0.032 fold) in primary kidney cells, but when these cells were pretreated (1h) with MG132 (a selective proteasome inhibitor²⁰, 0.5–5 μ M) or novel NF- κ B inhibitors (Supplementary Fig. 11^{21,22} 5 μ M), Ngal-Luc2 activity was inhibited 15–100% in a dose-dependent manner. For example, novel compound A reduced NGAL-Luc2 expression to 0.27±0.002 fold (Fig. 5b). These results indicate that NF- κ B plays an important role in *Ngal* regulation.

Because primary kidney cultures contain cells from many parts of the nephron, we examined whether lipid A-responsive, Ngal-Luc2 expression originated from cortical or medullary tubular cells. Cortical and medullary regions of the reporter kidneys were dissected and quantification of *Aquaporin1* (marker for proximal tubules), *Aquaporin2* and *Uromodulin* (markers for distal tubules and collecting ducts, respectively) by QPCR validated the dissection (Fig. 5c). When these two pools of cells were treated with lipid A (4 μ g/ml), medullary cells demonstrated intensive Ngal-Luc2 expression compared with the cortical population (4.48 $\times 10^4 \pm 5.24 \times 10^3$ photon/mg total protein vs 1.26 $\times 10^4 \pm 2.49 \times 10^3$ photon/mg total protein, respectively; Fig. 5d). These data confirm that medullary cells upregulate Ngal-Luc2 in respond to bacteria and lipid A.

Discussion

The *Ngal* promoter was selected to detect cellular stress and injury because a large body of literature shows that Ngal is intensely expressed subsequent to injury of humans and animals^{5, 6, 8, 9, 23}. Ngal protein appears early in the course of disease, anticipating the diagnosis of AKI⁸ and even patient death^{6, 24, 26}. In the injury, Ngal is essential in defense against bacterial invasion, by restricting iron traffic²⁷. Each of these characteristics suggested that the endogenous promoter and its 5'UTR may be useful to visualize injury by placing *Luc2/mC* under their control.

Using the reporter mouse, we tested the relationship between kidney and urine Ngal in real time because Ngal-*Luc2/mC* could be quantified in individual organs and since *Luc2/mC* lacked signal sequences it accumulated in injured cells. We found that (1), the timing and the intensity of kidney Ngal-*Luc2/mC* and uNgal were correlated; (2), both kidney NGAL-*Luc2/mC* and uNgal were dependant on the dose of injury; (3), the kidney was the principal or the only site of *Luc2/mC* expression in careful unilateral or bilateral surgeries and consequently uNgal production derived from the kidney; (4), TAL and CD cells activated *Ngal-Luc2/mC* *in vitro* and *in vivo* in response to the same stressors, implying that uNgal derived in a cell autonomous manner; (5), the expression of *Ngal-Luc2/mC* in segmental ischemia implied that uNgal was an autonomous feature of the damaged nephron or the result of localized signaling among damaged nephrons; (6) uNgal was independent of sNgal, since *Ngal*^{-/-} hosts implanted with *Ngal*^{+/+} kidneys generated uNgal; (7) kidney *Ngal* was unaffected by neutrophil deletion. We conclude that kidney *Ngal* generated uNgal. In contrast, a small amount of sNgal may reach the urine⁵ from the liver¹⁷, neutrophils¹⁴ or perhaps from the kidney itself (as demonstrated in cross-transplants, data not shown) escaping degradation in proximal tubules⁵ (**Model**: Supplementary Fig. 12).

The reporter mice also demonstrated that the activation of the *Ngal* gene was more sensitive and rapid than the accumulation of sCr, and it was independent of the complexities of uCr measurements¹⁰. For example, unilateral or segmental kidney ischemia or low doses of lipid A were detected by *NGAL-Luc2/mC* reporters even while the majority of the kidney was unaffected and sCr unchanged. Additionally, *Ngal-Luc2/mC* could detect kidney injury as early as 3–6h after its onset and by 12h distinguish different doses of ischemia, whereas sCr was statistically elevated only 12h after bilateral ischemic kidney damage. In this light, Ngal expression might detect the earliest stage of renal injury caused by medications²³ or by

diseases which may otherwise be clinically silent (e.g. early sepsis, unilateral obstructive uropathy) and *Ngal-Luc2/mC* may also be useful to monitor therapies which mitigate kidney injury²⁸. For example, *Ngal-Luc2/mC* is suppressed when the pathway is interrupted upstream by antibiotics and downstream by NF- κ B inhibitors.

The TAL and CD were unexpected sources of uNgal, but then again these segments are known to respond to various forms of AKI (Reviewed by Heyman)²⁹. Dilation and flattening of the epithelia, activation of apoptotic pathways⁴ and the shedding of cells (especially α -intercalated cells)^{30,31} are characterized in these segments. However, compared with the proximal tubule, damage appears to be mitigated by growth factors³², HIF^{29,33} and ERK and the redistribution of corticomedullary circulation³⁴. In fact, Ngal expressing cells in the TAL and CD did not appear apoptotic (Supplementary Fig. 9). Hence, while responding to a number of insults, the survival of the TAL and CD may permit them to “report” nephron injury by expressing Ngal whereas necrosis of proximal segments may render this compartment a more variable source for measuring a *de novo* genetic response.

Here we report a technique to evaluate inherent features of a candidate biomarker to report cell stress and injury *in vivo*, in real time, at the site of injury. The *Ngal-Luc2/mC* mouse authenticated the quantitative linkage between cell stress, kidney *Ngal* and uNgal. We propose that this analysis may be generally required to authenticate the use of a biomarker. For example, while cardiac troponin and kidney Ngal may both quantify the degree of injury (the prospective infarct size³⁵ or RIFLE score^{8,36}) and predict clinical outcomes (cardiac death³⁷ or renal replacement therapy^{6,24,26,36}), the two markers are dissimilar in that troponin is a pre-formed protein which is released from injured cells, while Ngal and other biomarkers require *de novo* expression and hence monitoring at the transcriptional level. These rigorous methods should also be applied to more complex models (e.g. pre-existing chronic kidney disease^{38,39}) where the ratio between organ and biofluid expression may vary from acute injury. We conclude that the *Ngal-Luc2/mC* mouse provides a non-invasive method of continuous and quantitative detection of gene expression *in vivo* permitting longitudinal assessment of organs undergoing stress.

Methods

Mouse husbandry

We used *Ngal-Luc2/mC*, *Ngal*^{-/-}, C57B6 mice according to approved protocols by Columbia IACUC.

Construction of pLuc2-mcherry di-fusion reporter gene

We PCR amplified Open reading frames (ORF) of Luciferase (*Luc2*, without stop codon) and mCherry (mC, with stop codon) from pGL4.10 (Promega) and pRSET-B-mCherry (Clontech), respectively using Pfu Ultra DNA polymerase (Stratagene) and primers shown in Supplementary Table 1. Overlapping PCR ligated their ORFs separated by a 42bp spacer to generate an in-frame *Luc2-mC* di-fusion reporter gene. We subcloned *Luc2/mC* di-fusion gene into pCI-neo (Promega) and verified its functional expression in HeLa cells.

Generation of a Ngal di-fusion reporter mouse

We constructed Ngal targeting BAC DNA by using modified BAC recombineering. BAC DNA clone (RP23-108C11, Children's Hospital Oakland Research Institute) was transformed into SW105 (NCI). The *Luc2/mC* di-fusion gene was cloned upstream of a LoxP1-Neo-LoxP1 cassette in the PL452 plasmid (NCI) and the *Luc2/mC-LNL* was PCR-amplified by using Expand High Fidelity *Taq* polymerase (Roche) and primers with an overhanging sequence of 75 nucleotides complementary to the flanking sequences of the knockin site located at the translation start site of the *Ngal* gene. We then electroporated *Luc2/mC-LNL* into BAC-containing SW105 cells and the kanamycin-resistance clones were verified by PCR and DNA sequencing. Similarly, a DTA-Amp^r cassette was recombineered to a site 2kb downstream of the *Luc2/mC-LNL* resulting in replacement of 1kb genomic DNA.

Columbia Transgenic Facility protocols were used for electroporation of *Ngal* targeting BAC DNA in KV1 ES cells (HICCC Transgenic Shared Resource, Columbia), neomycin selection, and PCR screening of neomycin-resistant ES clones for homologous recombination (Supplementary Table 1). KV1 ES cells were developed from C57BL6/129 hybrid mouse blastocysts in the Columbia Transgenic Facility and are commonly used to generate knockout mice at Columbia. Approximately 8% of ES cell clones were correctly targeted by homologous recombination at both 5' and 3' arms flanking the knockin site. We PCR-genotyped the *Ngal-Luc2/mC* di-fusion reporters (Supplementary Table 1). *Ngal-Luc2/mC* heterozygous C57BL/6 mice developed normally without a defective phenotype.

Bioluminescence and fluorescence imaging of *Ngal-Luc2/mC* reporter mice

We injected *Ngal-Luc2/mC* reporter mice *i.p.* with 150 mg/kg of D-Luciferin in PBS (pH 7.0). Ten minutes later, the mice are anesthetized (2.5% isofluorane) and a whole body image was acquired for 30s using the Xenogen IVIS optical imaging system (Caliper Life Sciences) with open excitation and emission filters for luminescence and fluorescence, respectively. Regions of interest (ROIs) were drawn on the dorsal side of the animal and quantified by using Living Image Software version 3.1⁴⁰. Counts in the ROIs were detected by a CCD camera digitizer and were converted to physical units of radiance in photons/s/cm²/steradian⁴⁰.

Isolation and culture of primary cells

We perfused *Ngal-Luc2/mC* mice (8-12wk of age) and dispersed the kidney cells with collagenase (2mg/ml; Sigma) for culture (1×10⁵/well Falcon) in DMEM/F12 medium supplemented with 10% FBS, 1% penicillin-streptomycin and 46mg/l L-Valine. Alternatively, we separated cortical and medullary domains and then isolated the primary cells from these regions.

We treated primary cells for 24 hours with 10⁴ CFU/ml *E. coli* (CFT073) and in some cases with 100µg/ml gentamicin, lipid A, and the NF-κB inhibitors MG132 (Cayman Chemical), Analogues 27, 30, and 31²² and Analogue 30²¹. The Luciferase substrate (Dual-Glo™ Luciferase Assay System; Promega) was added and luminescence from Luc2 and

fluorescence from mC (excitation of 500–550nm and emission of 575–650nm) were imaged in a Xenogen IVIS optical imaging system.

***In situ* hybridization, immunohistochemistry, western blot**

We analyzed frozen and paraffin-embedded mouse kidneys and urinary samples by standard procedures (please see **Supplementary Methods**).

Real-time PCR analysis

We isolated total RNA with the mirVANA RNA extraction kit (Ambion), and the first strand cDNA was synthesized by using Superscript III (Invitrogen). We performed real-time PCR to quantify *Ngal*, *Kim1*, *Aqp1*, *Aqp2*, and *Umod* mRNA expression in an iCycler MyiQ (Bio-Rad) with a SBR green Supermix reagent (Bio-Rad) and specific primers (Supplementary Table 1). β -actin was quantified as an internal control. $\Delta\Delta CT$ was used to calculate fold amplification of transcripts.

Neutrophil ablation

We introduced mAb RB6-8C5 (rat anti-mouse IgG2b; *i.p.* 150 μ g), which depletes mouse neutrophils and eosinophils 24h before ischemia. Control mice received 150 μ g of rat IgG2b (Sigma). FACs utilized FITC-conjugated RB6-8C5⁴¹.

Kidney ischemia and cross transplantation

We used vascular clamps or surgical threads for renal artery ischemia (15 or 30min). We identified the ischemic dose in wild type kidneys. Bilateral renal ischemia used an abdominal approach that required displacing liver and spleen (which may have induced *Ngal-Luc2* expression) as opposed to unilateral ischemia that used a flank incision. We used previously reported surgical procedures⁴² for cross-transplant (please see **Supplementary Methods**). Each animal was monitored for two weeks until sCr stabilized to 0.4 mg/dL and uNgal was essentially undetectable, prior to 10min ischemia to the transplanted kidney.

Supplementary Material

Refer to Web version on PubMed Central for supplementary material.

Acknowledgements

We are grateful for the advice of Q. Al-Awqati and J. A. Oliver. This work was supported by a grant from the Office of Columbia University Technology Ventures. J.B., N.P., and A.Q. are supported by grants from the National Institute of Diabetes and Digestive and Kidney Diseases (DK-55388 and DK-58872) and the March of Dimes for Birth Defects. Additional funding to J.B. was provided by the Glomerular Center of Columbia University.

References

1. Bosch JP, et al. Renal functional reserve in humans. Effect of protein intake on glomerular filtration rate. *The American journal of medicine*. 1983; 75:943–950. [PubMed: 6650549]
2. Lassnigg A, et al. Minimal changes of serum creatinine predict prognosis in patients after cardiothoracic surgery: a prospective cohort study. *Journal of the American Society of Nephrology : JASN*. 2004; 15:1597–1605. [PubMed: 15153571]

3. Christensen EI, Verroust PJ. Interstitial fibrosis: tubular hypothesis versus glomerular hypothesis. *Kidney international*. 2008; 74:1233–1236. [PubMed: 18974759]
4. Supavekin S, et al. Differential gene expression following early renal ischemia/reperfusion. *Kidney international*. 2003; 63:1714–1724. [PubMed: 12675847]
5. Mori K, et al. Endocytic delivery of lipocalin-siderophore-iron complex rescues the kidney from ischemia-reperfusion injury. *J Clin Invest*. 2005; 115:610–621. [PubMed: 15711640]
6. Nickolas TL, et al. Sensitivity and specificity of a single emergency department measurement of urinary neutrophil gelatinase-associated lipocalin for diagnosing acute kidney injury. *Ann Intern Med*. 2008; 148:810–819. [PubMed: 18519927]
7. Bennett M, et al. Urine NGAL predicts severity of acute kidney injury after cardiac surgery: a prospective study. *Clin J Am Soc Nephrol*. 2008; 3:665–673. [PubMed: 18337554]
8. Mishra J, et al. Identification of neutrophil gelatinase-associated lipocalin as a novel early urinary biomarker for ischemic renal injury. *J Am Soc Nephrol*. 2003; 14:2534–2543. [PubMed: 14514731]
9. Barasch J, Mori K. Cell biology: iron thievery. *Nature*. 2004; 432:811–813. [PubMed: 15602535]
10. Waikar S, Sabbiseti VS, Bonventre J. Normalization of urinary biomarkers to creatinine during changes in glomerular filtration rate. *Kidney international*. 2010:1523–1755.
11. Mishra J, et al. Neutrophil gelatinase-associated lipocalin (NGAL) as a biomarker for acute renal injury after cardiac surgery. *Lancet*. 2005; 365:1231–1238. [PubMed: 15811456]
12. Ramphal R, et al. Control of *Pseudomonas aeruginosa* in the lung requires the recognition of either lipopolysaccharide or flagellin. *Journal of immunology (Baltimore, Md : 1950)*. 2008; 181:586–592.
13. Li X, Hassoun HT, Santora R, Rabb H. Organ crosstalk: the role of the kidney. *Current opinion in critical care*. 2009; 15:481–487. [PubMed: 19851101]
14. Klausen P, Niemann CU, Cowland JB, Krabbe K, Borregaard N. On mouse and man: neutrophil gelatinase associated lipocalin is not involved in apoptosis or acute response. *Eur J Haematol*. 2005; 75:332–340. [PubMed: 16146540]
15. Chassin C, et al. Renal collecting duct epithelial cells react to pyelonephritis-associated *Escherichia coli* by activating distinct TLR4-dependent and - independent inflammatory pathways. *Journal of immunology (Baltimore, Md : 1950)*. 2006; 177:4773–4784.
16. El-Achkar TM, et al. Sepsis induces changes in the expression and distribution of Toll-like receptor 4 in the rat kidney. *Am J Physiol Renal Physiol*. 2006; 290:F1034–1043. [PubMed: 16332927]
17. Flo TH, et al. Lipocalin 2 mediates an innate immune response to bacterial infection by sequestering iron. *Nature*. 2004; 432:917–921. [PubMed: 15531878]
18. Brzuszkiewicz E, et al. How to become a uropathogen: comparative genomic analysis of extraintestinal pathogenic *Escherichia coli* strains. *Proceedings of the National Academy of Sciences of the United States of America*. 2006; 103:12879–12884. [PubMed: 16912116]
19. Cowland JB, Sorensen OE, Sehested M, Borregaard N. Neutrophil gelatinase-associated lipocalin is up-regulated in human epithelial cells by IL-1 beta, but not by TNF-alpha. *J Immunol*. 2003; 171:6630–6639. [PubMed: 14662866]
20. Chen Z, et al. Signal-induced site-specific phosphorylation targets I kappa B alpha to the ubiquitin-proteasome pathway. *Genes & development*. 1995; 9:1586–1597. [PubMed: 7628694]
21. Gong G, et al. Discovery of novel small molecule cell type-specific enhancers of NF-kappaB nuclear translocation. *Bioorg Med Chem Lett*. 2009; 19:1191–1194. [PubMed: 19136257]
22. Xie Y, et al. Identification of N-(quinolin-8-yl)benzenesulfonamides as agents capable of down-regulating NFkappaB activity within two separate high-throughput screens of NFkappaB activation. *Bioorg Med Chem Lett*. 2008; 18:329–335. [PubMed: 18024113]
23. Mishra J, et al. Neutrophil gelatinase-associated lipocalin: a novel early urinary biomarker for cisplatin nephrotoxicity. *Am J Nephrol*. 2004; 24:307–315. [PubMed: 15148457]
24. Haase-Fielitz A, et al. The predictive performance of plasma neutrophil gelatinase-associated lipocalin (NGAL) increases with grade of acute kidney injury. *Nephrol Dial Transplant*. 2009; 24:3349–3354. [PubMed: 19474273]

25. Hall IE, et al. IL-18 and urinary NGAL predict dialysis and graft recovery after kidney transplantation. *Journal of the American Society of Nephrology : JASN*. 21:189–197. [PubMed: 19762491]
26. Kùmpers P, H C, Lukasz A, Lichtinghagen R, Brand K, Fliser D, Faulhaber-Walter R, Kielstein JT. Serum neutrophil gelatinase-associated lipocalin at inception of renal replacement therapy predicts survival in critically ill patients with acute kidney injury. *Critical care (London, England)*. 2010; 14(1):R9.
27. Goetz DH, et al. The neutrophil lipocalin NGAL is a bacteriostatic agent that interferes with siderophore-mediated iron acquisition. *Mol Cell*. 2002; 10:1033–1043. [PubMed: 12453412]
28. Haase M, et al. Sodium bicarbonate to prevent increases in serum creatinine after cardiac surgery: a pilot double-blind, randomized controlled trial. *Critical care medicine*. 2009; 37:39–47. [PubMed: 19112278]
29. Heyman S, Rosenberger C, Rosen S. Experimental ischemia-reperfusion: biases and myths—the proximal vs. distal hypoxic tubular injury debate revisited. *Kidney international*. 2009 2009/09/16/online.
30. Han K-H, et al. Effects of ischemia-reperfusion injury on renal ammonia metabolism and the collecting duct. *American journal of physiology Renal physiology*. 2007; 293:F1342–1354. [PubMed: 17686949]
31. Srichai MB, et al. Apoptosis of the thick ascending limb results in acute kidney injury. *Journal of the American Society of Nephrology : JASN*. 2008; 19:1538–1546. [PubMed: 18495962]
32. di Mari JF, Davis R, Safirstein RL. MAPK activation determines renal epithelial cell survival during oxidative injury. *The American journal of physiology*. 1999; 277:F195–203. [PubMed: 10444573]
33. Rosenberger C, et al. Adaptation to hypoxia in the diabetic rat kidney. *Kidney international*. 2008; 73:34–42. [PubMed: 17914354]
34. Brezis M, Rosen S. Hypoxia of the renal medulla—its implications for disease. *The New England journal of medicine*. 1995; 332:647–655. [PubMed: 7845430]
35. Steen H, et al. Cardiac troponin T at 96 hours after acute myocardial infarction correlates with infarct size and cardiac function. *J Am Coll Cardiol*. 2006; 48:2192–2194. [PubMed: 17161244]
36. Haase M, Bellomo R, Devarajan P, Schlattmann P, Haase-Fielitz A. Accuracy of neutrophil gelatinase-associated lipocalin (NGAL) in diagnosis and prognosis in acute kidney injury: a systematic review and meta-analysis. *American journal of kidney diseases : the official journal of the National Kidney Foundation*. 2009; 54:1012–1024. [PubMed: 19850388]
37. Newby LK, et al. The GUSTO-IIa Investigators. Value of serial troponin T measures for early and late risk stratification in patients with acute coronary syndromes. *Circulation*. 1998; 98:1853–1859. [PubMed: 9799204]
38. Bolignano D, et al. Neutrophil gelatinase-associated lipocalin in patients with autosomal-dominant polycystic kidney disease. *American journal of nephrology*. 2007; 27:373–378. [PubMed: 17570904]
39. Damman K, et al. Both in- and out-hospital worsening of renal function predict outcome in patients with heart failure: results from the Coordinating Study Evaluating Outcome of Advising and Counseling in Heart Failure (COACH). *Eur J Heart Fail*. 2009; 11:847–854. [PubMed: 19696057]
40. Rice BW, Cable MD, Nelson MB. In vivo imaging of light-emitting probes. *J Biomed Opt*. 2001; 6:432–440. [PubMed: 11728202]
41. Lysenko ES, Ratner AJ, Nelson AL, Weiser JN. The role of innate immune responses in the outcome of interspecies competition for colonization of mucosal surfaces. *PLoS Pathog*. 2005; 1:e1. [PubMed: 16201010]
42. Zhang Z, et al. Improved techniques for kidney transplantation in mice. *Microsurgery*. 1995; 16:103–109. [PubMed: 7783600]
43. Kollisch G, et al. Various members of the Toll-like receptor family contribute to the innate immune response of human epidermal keratinocytes. *Immunology*. 2005; 114:531–541. [PubMed: 15804290]

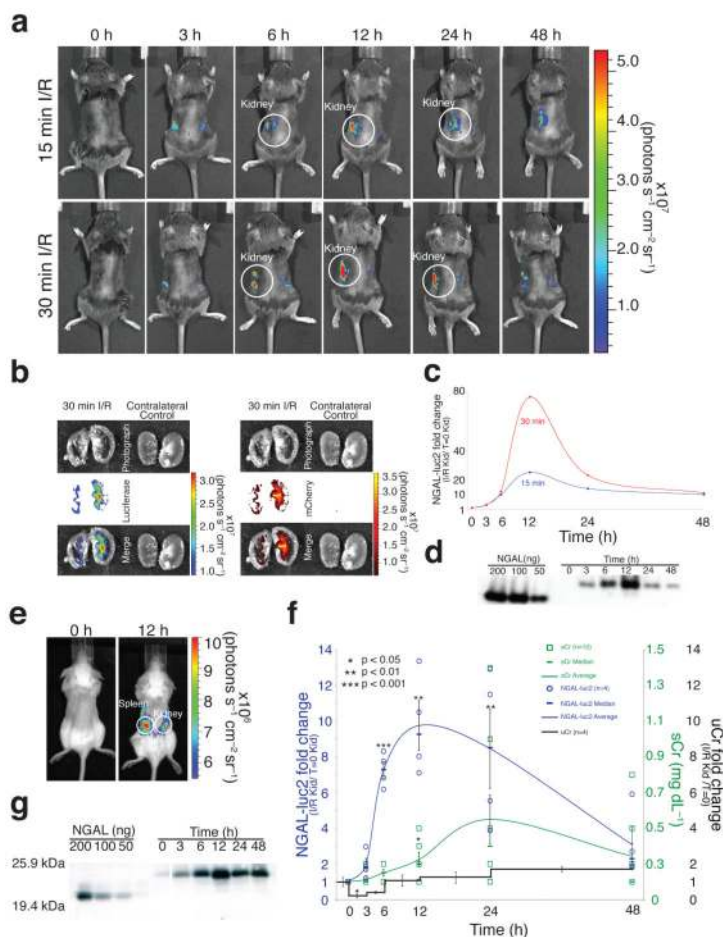


Figure 1.

Ngal-Luc2/mC visualized kidney damage in real time *in vivo*. (a) Heterozygous *Ngal-Luc2/mC* female mice were subjected to left kidney ischemia for 15 (top panel) or 30min (bottom panel) and visualized in a Bioimager (30s). *Ngal-Luc2* was nearly specific to the left kidney. (b) *Ngal-Luc2/mC* radiated from the medulla 12h after injury, but not from the contralateral, uninjured kidney. (c) Photon emission (Panel A) was plotted by subtracting background radiance of the contralateral kidney, and normalizing the data for luminescence at 0h. The average radiance ($\text{ps}^{-1}\text{cm}^{-2}\text{sr}^{-1}$) within a constant region of interest (ROI) was converted to fold change and displayed on the Y-axis. (d) Immunoblot detection of uNgal from the ischemic mouse (15min) shown in Panel A. Recombinant mouse non-glycosylated *Ngal* was used as a standard. (e) Heterozygous *Ngal-Luc2/mC* albino female mice were subjected to bilateral ischemia for 15min and *NGAL-Luc2* was examined 12h later. (f) *Ngal-Luc2* activity rose significantly by 6h after 15min of ischemia (compared to time=0: $t=3\text{h}$, $P=0.085$; $t=6\text{h}$, $P=0.0009$; $t=12\text{h}$, $P=0.008$; $t=24\text{h}$, $P=0.04$; $t=48\text{h}$, $P=0.12$; $n=4$), while a significant elevation of sCr lagged until 12h (compared to time=0: $t=3\text{h}$, $P=0.35$; $t=6\text{h}$, $P=0.18$; $t=12\text{h}$, $P=0.028$; $t=24\text{h}$, $P=0.055$; $t=48\text{h}$, $P=0.15$; $n=10$). uCr fell within a narrow interval (baseline vs: 0-3h, 0.22 fold, $P=0.027$; 3-6h, 0.41 fold, $P=0.15$), then returned to steady state (baseline vs: 6-12h, 1.08 fold, $P=0.31$; 12-24h, 1.27 fold, $P=0.19$; 24-48h, a

1.22 fold change $p=0.15$). Median \pm s.e. (g) uNgal protein from the mouse in Panel E paralleled the expression of kidney Ngal-Luc2.

Author Manuscript

Author Manuscript

Author Manuscript

Author Manuscript

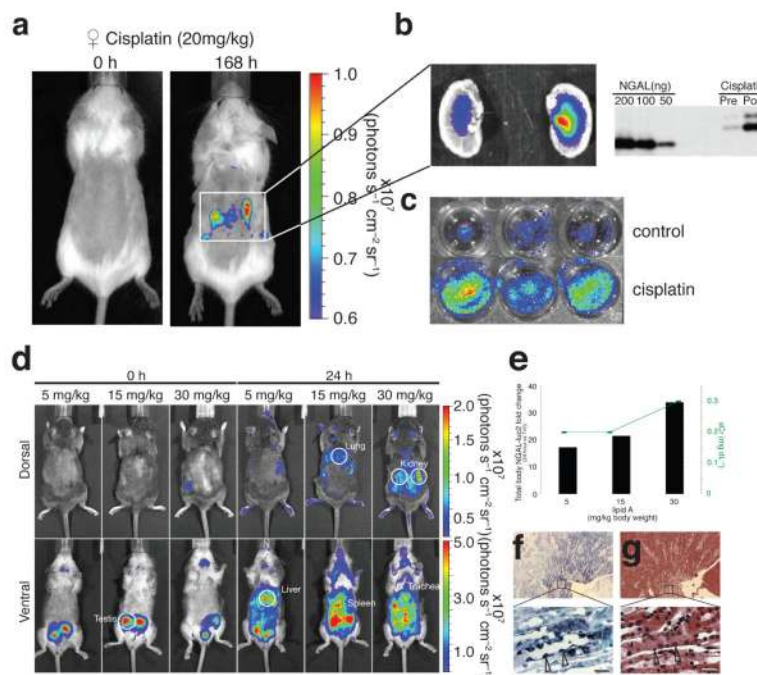


Figure 2. *Ngal-Luc2/mC* reported kidney cellular damage *in vivo*, which was induced by cisplatin and lipid A. **(a)** *Ngal-Luc2/mC* expression in both kidneys of a mouse 168h after cisplatin (20 mg/kg) exposure. **(b)** Treated kidneys revealed prominent *Ngal-Luc2/mC* expression in the medulla and abundant uNgal. **(c)** *Ngal-Luc2/mC* kidney cells responded to cisplatin (10 μ M). **(d)** *Ngal-Luc2/mC* fluorescence was elicited by lipid A in a dose-dependent manner in the kidney, liver, spleen, lung and trachea. Low level expression of *Ngal-Luc2/mC* is also seen in the skin of the feet, consistent with expression of TLR4⁴³. **(e)** 5, 15 and 30 mg/Kg of lipid A led to a 17, 21 and 34 fold increase in total *Ngal*-reporter expression after 24h ($n=3$). sCr is shown for each dose. **(f)** *In situ* hybridization demonstrated *Ngal* mRNA in TAL and CD in the outer stripe of the inner medulla. **(g)** H&E staining revealed cast formation 24h after a 5 mg/kg lipid A challenge. High magnification images of the delineated regions (**f** and **g**) showed that *Ngal* RNA was localized to presumptive intercalated cells (open arrowhead) of CDs that contained casts and cellular debris (asterisks).

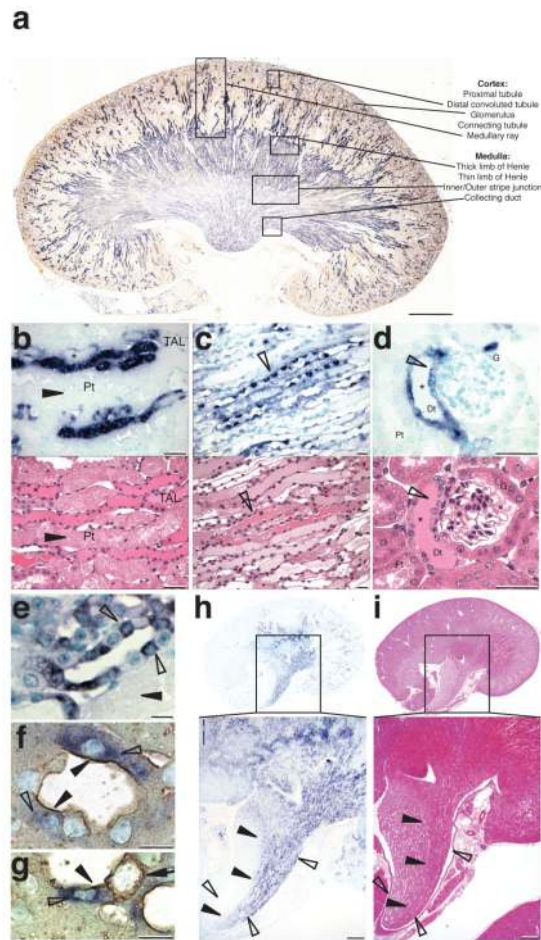


Figure 3. Damaged nephron is the source of kidney Ngal. **(a)** *In situ* hybridization shows *Ngal* mRNA expression in TAL and CD, weaker expression in distal convoluted tubules and absent expression in proximal tubules and thin limbs of Henle. **(b)** *Ngal* mRNA was expressed in the outer stripe of the outer medulla and cortical TAL of Henle (in medullary rays) containing casts (asterisks), in CD (open arrowheads) containing casts (asterisks, **c**), and the macula densa (open arrowhead) which had undergone epithelial flattening and cast formation (asterisks, **d**), but not in the necrotic pars recta of proximal tubules (closed arrowhead, **b** and **e**). Top panels show *in situ* hybridization and the bottom panels show H&E staining in paraffin sections. **(e)** High magnification image revealed that *Ngal* mRNA was specifically expressed by intercalated cells (open arrowheads). **(f)** Anti v-ATPase IHC identified *Ngal* expressing (open arrowhead) CD cells as α -type intercalated cells (α -IC) in which the v-ATPase locates to the apical surface (closed arrowhead). **(g)** Outer medullary CD expressed *Ngal* mRNA (open arrowhead) in α -IC cells, while adjacent β -type intercalated cells (closed arrow) failed to express NGAL. **(h, i)** A polar (segmental) renal artery was subjected to 30min ischemia, and after 24h, *Ngal* mRNA expression was located by *in situ* hybridization. *Ngal* mRNA (**h**) was expressed in the ischemic zone (**i**) where histological damage was evident (closed arrowheads). Closed arrowheads indicate the

boundary of damaged and non-damaged tubules in the papilla, and open arrowheads depict the width of the papilla.

Author Manuscript

Author Manuscript

Author Manuscript

Author Manuscript

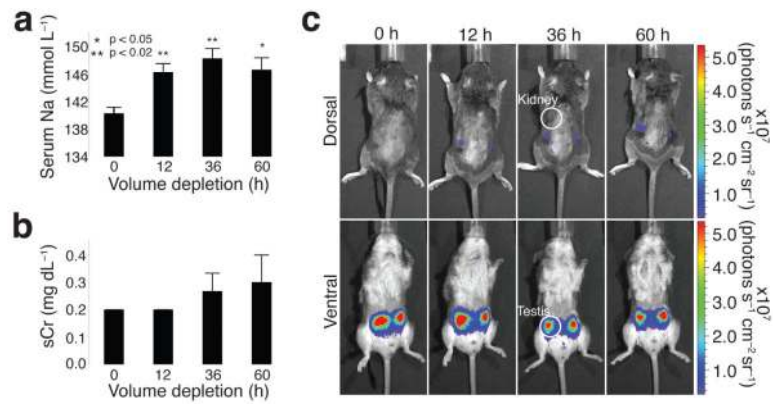


Figure 4.

Volume depletion failed to activate Ngal-reporter expression. **(a, b)** Volume depletion induced mild hypernatremia (serum sodium increased on average $8 \text{ mmol/L} \pm 2.5 \text{ s.e.}$ ($n=3$, * $P < 0.05$; ** $P < 0.02$), **(b)** mild azotemia with a rise in sCr to $0.3 \pm 0.2 \text{ s.e.}$ ($n=3$), and approximately a $21.7 \pm 4\%$ weight loss. **(c)** NGAL-Luc2 was not upregulated in any organ (the kidney is circled) following simple volume depletion. Male mice tonically express Ngal in testis (circled), which serves as an internal positive control.

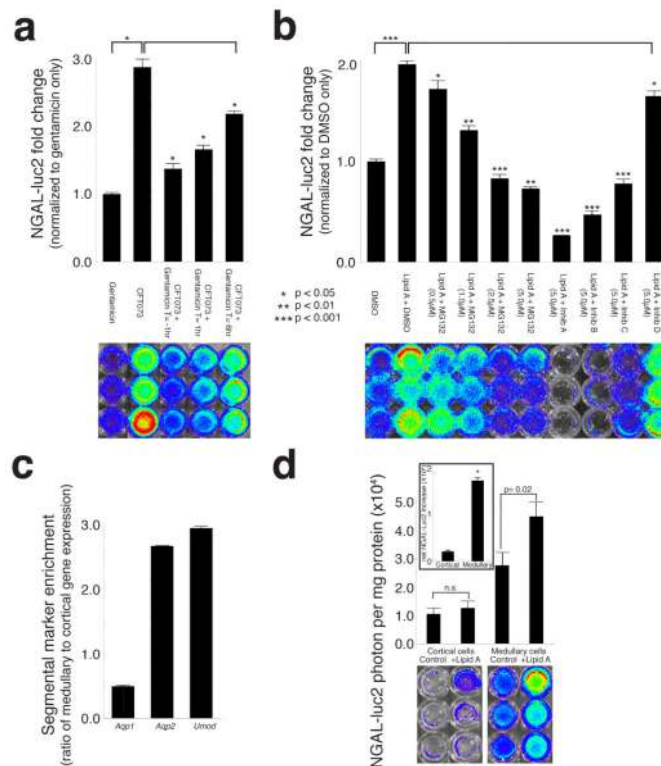


Figure 5.

(a) Uropathogenic *E. coli* (CFT073; 10^4 CFU/ml) and lipid A stimulate Ngal-Luc2 expression in primary kidney cells (10^5 cells/well) isolated from reporter mice. When these cells were pre-treated (1h) or post-treated (1 and 6h) with gentamicin (100 μ g/ml), there was a significant reduction in Ngal-Luc2 expression compared to the uninhibited growth ($n=3$, two independent experiments), pretreatment being more effective. (b) Ngal-Luc2 activity was induced by lipid A (4 μ g/ml), but pretreatment with either a known NF- κ B inhibitor, MG132 (0.5-5 μ M), or novel NF- κ B inhibitors (5 μ M) reduced Ngal-Luc2 activity by 15-80%. (* $P<0.05$, ** $P<0.01$, *** $P<0.001$; Student's t-Test two-tailed unequal variance; $n=3$ independent experiments). Bars represent fold change from DMSO control \pm s.e. (c) Primary cells isolated from the inner medulla and papilla of *Ngal-Luc2/mC* kidneys ($n=6$) demonstrated enrichment of distal tubular markers *Aqp2* and *Umod* and de-enrichment of *Aqp1*, a proximal tubular marker. Bars represent the ratio of gene expression (medullary vs cortical) \pm s.e. (d) Ngal-Luc2 expression was markedly increased by lipid A (4 μ g/ml, 24h) in inner medullary and papillary primary cells (Luc2 increased by $17.2 \times 10^3 \pm 6.14 \times 10^2$ photon/mg protein), but not in the cortical primary cells (increase of $2.11 \times 10^3 \pm 0.61 \times 10^3$ photon/mg protein). Bars represent total photon/mg protein and inset is the net change in photon/mg protein from the control \pm s.e.